Determination of the Degradation Pattern of Pump Using Two-Phase Diagnostic Bond Graph

Sumanta Kumar Dutta, Sawan Kumar, Tushar Kanti Saha and Sanjoy Kumar Ghoshal

Abstract A bond graph-based approach has been applied for failure prognosis in the hydraulic circuit. The degradation function of a fault in the system is determined using a two-phase diagnostic bond graph model (DBG). By intentionally imparting a time-varying fault in the pump displacement, the capability of the DBG model is exhibited. The analytical redundancy relations (ARRs) evaluated from the first DBG helps to discern the manifestation of fault. Making use of ARRs of the first phase, the second DBG delivers the degradation pattern of the fault enabling the determination of remaining useful life (RUL) of the system.

Keywords DBG · RUL · ARRs

1 Introduction

Fault detection and isolation (FDI) is an important tool for ensuring the safety, efficiency, and reliability of the system. Wu et al. [1] have discussed various techniques of energy savings. Lin et al. [2] have discussed different techniques of FDI. The overall system efficiency depends upon the robustness of the system, which is only achievable with proper fault detection of the system. Determination of FDI with a quantitative approach necessitates the generation of a mathematical model of the system. Use of the different constraints, different compatibility conditions have been presented in terms of known variables using the residual relations which are dubbed as analytical redundancy relations (ARRs) [3–5]. Making use of bond graph model of the system, FDI is able to identify the cause and type of fault and also the necessary measures which need to be taken to control the impact of these faults based on analytical redundancy approach.

But FDI comes into the fray after the occurrence of the fault, and in some cases, it is unable to control the degradation of the fault. In such instances, determining the time to failure (TTF) and remaining useful life (RUL), with help of prognostics, play

S. K. Dutta (✉) · S. Kumar · T. K. Saha · S. K. Ghoshal
Department of Mechanical Engineering, IIT(ISM) Dhanbad, Dhanbad, India
e-mail: dutta.sumantakr@gmail.com

H. Kumar and P. K. Jain (eds.), *Recent Advances in Mechanical Engineering*,
Lecture Notes in Mechanical Engineering,
https://doi.org/10.1007/978-981-15-1071-7_40

a significant hand in estimating the duration for which the system can be run safely until complete failure. But in order to evaluate the RUL, knowledge of the degradation pattern with time is paramount. Ascertaining the RUL of a system can be carried using either one of data-based or model-based approach. Model-based diagnostics approach is required for precise and infallible models of actual physical systems which incorporate several domains (such as mechanical, electrical, and hydraulic). Model-based methods require an accurate mathematical model that describes the expected behavior of the system. Whereas the data-based approach is governed by on the availability of a database of the performance of the system. But either approach has its fair share of shortcomings. To overcome these limitations, Borutzky [6] has proposed a method involving the use of two-phase diagnostic bond graphs (DBG) to assess the time-varying degradation behavior of the fault. The first-phase DBG is used to identify the appearance of a fault. Using the DBG, the ARRs are determined and from these adaptive thresholds are generated by taking into consideration the uncertainty associated with the value of parameters. The number of sensors determines the number of residuals generated. The fault signature matrix (FSM), which assists in the identification of the faulty components, is generated using the ARRs. Whenever any of the residuals crosses the adaptive thresholds, it signals the manifestation of fault [7]. After the identification of the source of the fault and its isolation, it is replaced by a time-varying parameter in the second phase of the DBG which gives the degradation behavior of fault. As time progresses, the residuals will head toward the failure limits. By inverting the ARRs, the time for this intersection can be computed which gives the RUL.

In this paper, the authors have considered a hydraulic circuit which has been described below. The two-phase DBG approach has been applied to the circuit for fault diagnosis and prognostics. To test the ability and applicability of the two-phase DBG method in accurately determining the deterioration pattern of the fault with time and hence establish the RUL of the system, a fault has been deliberately introduced in the displacement volume of the variable displacement pump.

The above-mentioned approach finds its utility in the various automated processes some of which are automated manufacturing processes, in which the absence of human supervision demands the early detection of fault occurrence and estimation of the remaining life. This helps in the prompt determination of the faulty component and its subsequent repairing and replacement preventing the breakdown of the machines and ensuring a reduced shutdown period, hence safeguarding the interests of the manufacturer by reducing the incurred costs.

The paper structure is as follows. The second section of this paper provides detailed information about the physical hydraulic system and its mathematical model. The second section houses the details of the behavioral and diagnostic model of the hydraulic system and its bond graph model. Section 3 explains in detail the two-phase DBG approach used in this work. Section 4 supplies the experimental results, and Sect. 5 provides a reasonable conclusion for the paper.

2 Diagnostic Bond Graph Approach

2.1 Parameter Degradation

It is assumed that the fault has occurred and has been isolated after being detected. The DBG approach is applied to the system to detect the degradation of the parameter. It is assumed that the parameter consists of two parts: the first is the nominal value which remains constant throughout, and second is the time-varying factor which degrades over time. Combined together, these two components give the overall value of the parameter which takes the system toward failure.

2.2 Determining the Degradation Function

Using the residuals along with the adaptive thresholds of the system, the occurrence of faults is detected, by the inspection of the FSM, by the first phase DBG. Taking the initially assumed value of the different parameters $g(t)$ from Table 2 and the outputs of the different sensors $h(t)$, the ARRs are generated. These ARRs provide the residuals $R^1(t)$ which act as fault identifiers. In the case of a fit system, i.e. if the actual value of the system parameter is distracted by their nominal values within the small acceptable range only, then ARR residuals are neighboring zero. If they exceed the appropriate definitive user-defined or adaptive thresholds, which account for parameters uncertainty, they indicate the beginning of a fault with a magnitude, which could potentially progress over time. ARR residuals may lie outside fault thresholds but inside failure alarm limits provided the parameter variates within certain limits. Hence, irrespective of the fact that a fault has occurred, a system continues operating with reduced efficiency and at a lower performance level for a time duration which depends upon how the faulty parameters degrade, the prediction of which is our objective. The second-phase DBG accounts for the unknown time-varying parameter degradation. Let Ø be the parameter and be the time-varying degradation parameter. Then, $Ø(t) = Ø_n + (t)$. If the latter is known and if measured outputs given by the faulty system are taken as inputs into the DBG of the second phase, then the evaluation of the ARRs will give residuals close to zero. To determine the RUL estimates, the available values of the fall function can be extended further. Extrapolation can be repeated with ongoing time and RUL estimates can be improved in this way (Fig. 1).

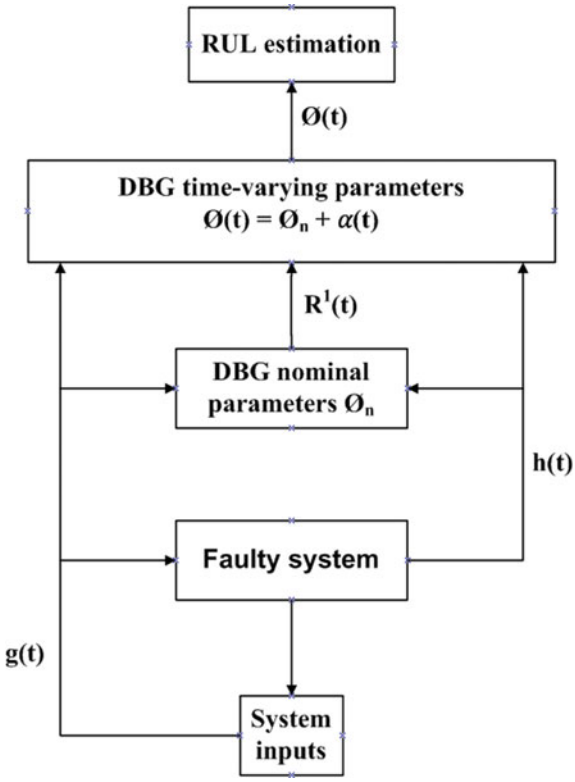

Fig. 1 Sequence of operation for determination of parameter degradation

3 The Hydraulic System

3.1 Physical Description of the System

The schematic representation of the setup being studied is shown in Fig. 2. Table 1 gives the names of the different components of setup corresponding to the tags given in Fig. 2. The setup has a double acting variable displacement pump (tag 2), driven by a 7.5 kW electric motor (tag 1), furnishing pressurized fluid to a bent axis hydro motor (tag 5). Before reaching the hydro motor, the fluid passes through a proportional flow control valve (tag 3), which is operated using a solenoid, which modulates the flow supplied to the hydro motor corresponding to the voltage imparted to the flow control valve. The hydro motor is used to drive a single-acting fixed displacement loading pump (tag 7) which in turn supplies fluid to the reservoir (tag 14.1–14.4) through a pressure relief valve (PRV) (tag 8). The load torque of the motor is regulated by varying the pressure setting of the PRV. The experiments are conducted on the setup under well-aerated conditions. To obtain fluid with constant viscosity at different parts of the setup, suitable oil cooler and filter are used. The oil cooler maintains the

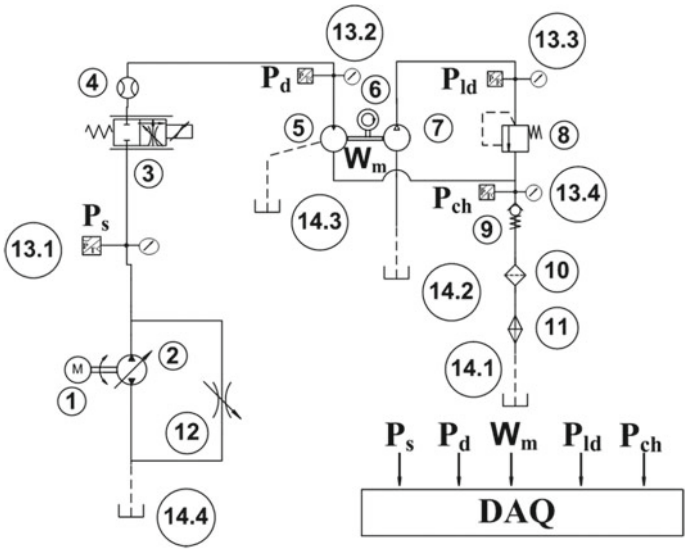

Fig. 2 Schematic representation of the setup

Table 1 Different components in the schematic diagram

Tag No.	Name of equipment
1	Electrical drive motor
2	Variable displacement pump
3	Proportional flow control valve
4	Flow sensor
5	Hydro motor
6	Speed sensor
7	Loading pump (fixed displacement)
8	Pressure relief valve
9	Spring-loaded check valve
10	Filter
11	Oil cooler
12	Flow restrictor valve
13.1–13.4	Pressure sensor
14.1–14.4	Hydraulic reservoir

temperature of the fluid in the range of 55–62 °C. The experimental setup has four pressure sensors (tag 13.1–13.4) and a speed sensor (tag 6) to measure the pressure at different sections of the system and the speed of the driven hydro motor which are recorded in the data acquisition system (DAQ). To ensure the accuracy of the setup, multiple test runs are conducted before collecting data.

3.2 The Bond Graph and Simulink Model of the System

The BG model of the hydraulic system is made with the storage elements having integrative causality. The system's Simulink model is prepared using this BG model.

According to the mathematical equations of the above section, a block model is made in MATLAB/Simulink. The model has been divided into two parts—Behavioral model and diagnostic model (Fig. 3). In the behavioral model, the constitutive relations given in Eqs. (1) through (5) are evaluated. Whereas, the diagnostic model is a simple computation of the residuals given in Eqs. (6) through (10) (Fig. 4).

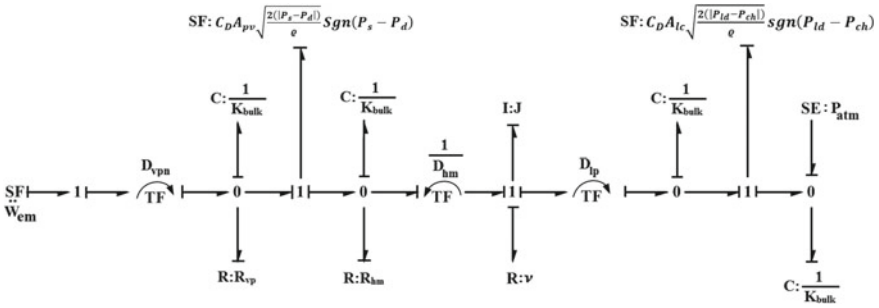

Fig. 3 Bond graph model of the hydraulic system

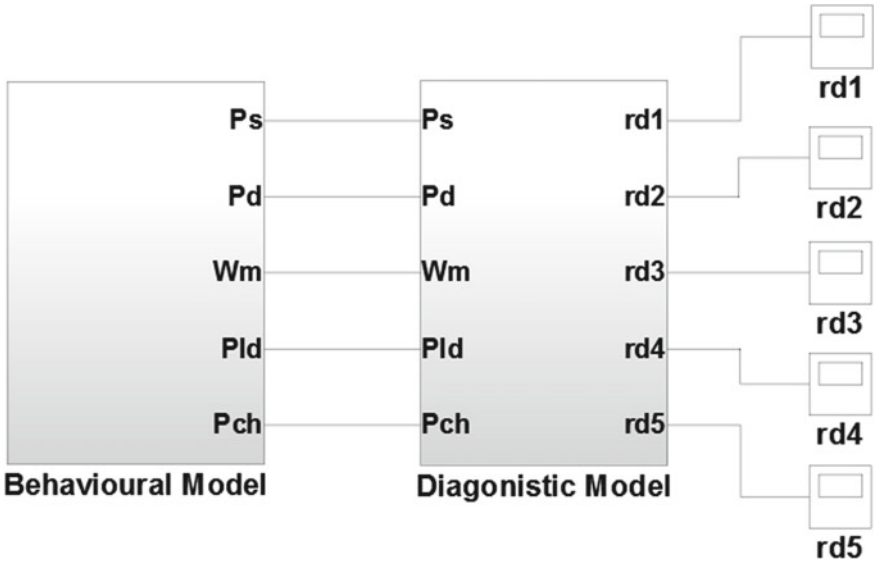

Fig. 4 Simulink model of the system

3.3 Mathematical Modeling of the System

The assumptions made for the mathematical modeling of the system are:

- Valve spool inertia and friction effects are not taken into consideration.
- Fluid does not get compressed while flowing through the pipes.
- The rate of flow through the flow control valve has a nonlinear relationship with the pressure differential across it.
- The fluid used in the system follows Newton's law of viscosity.

The mathematical equations for the different components in the system are derived with the combined use of bond graph and Simulink model.

Variable Displacement Pump

The volume flow rate lost due to compression in the variable pump can be mathematically given as

$$Q_{\mathrm{vp}} = D_{\mathrm{vp}}\omega_{\mathrm{em}} - \frac{P_{\mathrm{s}}}{R_{\mathrm{vp}}} - \left(C_{\mathrm{D}}A_{\mathrm{pv}}\sqrt{\frac{2(|P_{\mathrm{s}} - P_{\mathrm{d}}|)}{\varrho}}\mathrm{sgn}(P_{\mathrm{s}} - P_{\mathrm{d}})\right) \tag{1}$$

where,

Q_{vp}	Volume flow rate provided by the pump
D_{vp}	Variable pump displacement
R_{vp}	Resistance to leakage in variable displacement pump
P_{s}	Main pump pressure or system pressure
C_{D}	Coefficient of discharge
A_{pv}	Orifice area of the proportional valve
ω_{em}	Rotational speed of the driving electric motor
P_{d}	Proportional relief valve pressure or delivery pressure $= k_{\mathrm{bulk}} \int Q_{\mathrm{hm}}\mathrm{d}t$
$P_{\mathrm{s}} = k_{\mathrm{bulk}} \int Q_{\mathrm{vp}}\mathrm{d}t$, k_{bulk}	Bulk Modulus.

Fixed Displacement Loading Pump

Loading pump which is coupled with the hydraulic motor also experiences some hydraulic losses during fluid flowing through the pump. Now, the flow from the pump is given as,

$$Q_{\mathrm{lp}} = D_{\mathrm{lp}}w_{\mathrm{m}} - \left(C_{\mathrm{D}}A_{\mathrm{lc}}\sqrt{\frac{2(|P_{\mathrm{ld}} - P_{\mathrm{ch}}|)}{\varrho}}\mathrm{sgn}(P_{\mathrm{ld}} - P_{\mathrm{ch}})\right) \tag{2}$$

A_{lc}	Orifice area of the load valve
P_{ld}	Discharge pressure of the loading pump
P_{ch}	Check valve pressure at loading circuit

ϱ Density of fluid
w_{m} Angular velocity of the hydraulic motor.

Driven Hydraulic Motor

The torque provided by the hydro motor is,

$$T_{\mathrm{hm}} = D_{\mathrm{hm}}(P_{\mathrm{d}} - P_{\mathrm{ch}}) - \nu w_{\mathrm{m}} - D_{\mathrm{lp}} P_{\mathrm{ld}} \tag{3}$$

where

ν Viscous friction coefficient
D_{lp} Loading pump displacement

$w_{\mathrm{m}} = \frac{\int T_{\mathrm{hm}} \mathrm{d}t}{\text{Motor Inertia}} = \frac{\int T_{\mathrm{hm}} \mathrm{d}t}{J}$

where the pressure at the inlet to the loading pump $= P_{\mathrm{ld}} = k_{\mathrm{bulk}} \int Q_{\mathrm{lp}} \mathrm{d}t$.

The volume flow rate lost due to compression in the hydraulic motor can be mathematically given as

$$Q_{\mathrm{hm}} = \left(C_{\mathrm{D}} A_{\mathrm{pv}} \sqrt{\frac{2(|P_{\mathrm{s}} - P_{\mathrm{d}}|)}{\varrho}} \mathrm{sgn}(P_{\mathrm{s}} - P_{\mathrm{d}}) \right) - D_{\mathrm{hm}} w_{\mathrm{m}} - \frac{P_{\mathrm{d}}}{R_{\mathrm{hm}}} \tag{4}$$

where,

Q_{hm} Volume flow rate lost due to compression in the hydraulic motor
D_{hm} Volumetric displacement of the hydraulic motor
R_{hm} Resistance to leakage in the hydraulic motor.

Now, flow to the tank from the motor can be described as,

$$Q_{\mathrm{hm1}} = D_{\mathrm{hm}} w_{\mathrm{m}} - \left(C_{\mathrm{D}} A_{\mathrm{chv}} \sqrt{\frac{2(|P_{\mathrm{ch}} - P_{\mathrm{atm}}|)}{\varrho}} \mathrm{sgn}(P_{\mathrm{ch}} - P_{\mathrm{atm}}) \right) + \left(C_{\mathrm{D}} A_{\mathrm{lc}} \sqrt{\frac{2(|P_{\mathrm{ld}} - P_{\mathrm{ch}}|)}{\varrho}} \mathrm{sgn}(P_{\mathrm{ld}} - P_{\mathrm{ch}}) \right) \tag{5}$$

where,

A_{chv} Orifice area of the check valve at load circuit
P_{atm} Atmospheric pressure.

And corresponding effort $= P_{\mathrm{ch}} = k_{\mathrm{bulk}} \int Q_{\mathrm{hm1}} \mathrm{d}t$.

Residuals

In this application, five sensors are used; therefore, the number of residuals will be five. In this section, the first-phase residuals have been determined along with the adaptive thresholds.

From Eq. (1), the first residual can be described as below,

$$rd_1 = D_{\mathrm{vp}}\omega_{\mathrm{em}} - \frac{\dot{P}_{\mathrm{s}}}{k_{\mathrm{bulk}}} - \left(\frac{P_{\mathrm{s}}}{R_{\mathrm{vp}}}\right) - \left(C_{\mathrm{D}}A_{\mathrm{pv}}\sqrt{\frac{2(|P_{\mathrm{s}} - P_{\mathrm{d}}|)}{\varrho}}\mathrm{sgn}(P_{\mathrm{s}} - P_{\mathrm{d}})\right) \tag{6}$$

and

$$\varepsilon_1 = \frac{|\dot{P}_{\mathrm{s}}|}{\delta k_{\mathrm{bulk}}} + \left(\delta D_{\mathrm{vp}}|\omega_{\mathrm{em}}|\right) + \left[\delta(C_{\mathrm{D}}A_{\mathrm{pv}})\right]\sqrt{\frac{2|P_{\mathrm{s}} - P_{\mathrm{d}}|}{\varrho}} + \frac{|P_{\mathrm{s}}|}{\delta R_{\mathrm{vp}}}$$

Here, δ is the uncertainty for the associated parameter and its value is considered as 0.1 (i.e. 10%).

Upper threshold value $= rd_1 + \varepsilon_1$
Lower threshold value $= rd_1 - \varepsilon_1$

From Eq. (2), the second residual can be described as below,

$$rd_2 = \frac{\dot{P}_{\mathrm{ld}}}{k_{\mathrm{bulk}}} - D_{\mathrm{lp}}w_{\mathrm{m}} + C_{\mathrm{D}}A_{\mathrm{lc}}\sqrt{\frac{2|P_{\mathrm{ld}} - P_{\mathrm{ch}}|}{\varrho}}\mathrm{sgn}(P_{\mathrm{ld}} - P_{\mathrm{ch}}) \tag{7}$$

and

$$\varepsilon_2 = \frac{|\dot{P}_{\mathrm{ld}}|}{\delta k_{\mathrm{bulk}}} + \left(\delta D_{\mathrm{lp}}|w_{\mathrm{m}}|\right) + \left[\delta(C_{\mathrm{D}}A_{\mathrm{lc}})\right]\sqrt{\frac{2|P_{\mathrm{ld}} - P_{\mathrm{ch}}|}{\varrho}}$$

Upper threshold value $= rd_2 + \varepsilon_2$
Lower threshold value $= rd_2 - \varepsilon_2$

According to Eq. (3), the third residual is as follows,

$$rd_3 = D_{\mathrm{hm}}(P_{\mathrm{d}} - P_{\mathrm{ch}}) - \nu w_{\mathrm{m}} - D_{\mathrm{lp}}P_{\mathrm{ld}} - J\dot{w}_{\mathrm{m}} \tag{8}$$

and

$$\varepsilon_3 = \delta D_{\mathrm{hm}}|P_{\mathrm{d}} - P_{\mathrm{ch}}| + (\delta\nu|w_{\mathrm{m}}|) + \left(\delta D_{\mathrm{lp}}|P_{\mathrm{ld}}|\right) + (\delta J|\dot{w}_{\mathrm{m}}|)$$

Upper threshold value $= rd_3 + \varepsilon_3$
Lower threshold value $= rd_3 - \varepsilon_3$

The fourth residual corresponding to the Eq. (4) is,

$$rd_4 = \left(C_D A_{pv}\sqrt{\frac{2(|P_s - P_d|)}{\varrho}}\,\mathrm{sgn}(P_s - P_d)\right) - D_{hm} w_m - \frac{\dot{P}_d}{k_{bulk}} - \frac{P_d}{R_{hm}} \tag{9}$$

and

$$\varepsilon_4 = \frac{|\dot{P}_d|}{\delta k_{bulk}} + (\delta D_{hm}|w_m|) + \left[\delta\left(C_D A_{pv}\right)\right]\sqrt{\frac{2|P_s - P_d|}{\varrho}} + \frac{|P_d|}{R_{hm}}$$

Upper threshold value $= rd_4 + \varepsilon_4$
Lower threshold value $= rd_4 - \varepsilon_4$

From Eq. (5), the fifth residual can be derived as,

$$\begin{aligned} rd_5 = D_{hm} w_m &- \left(C_D A_{chv}\sqrt{\frac{2(|P_{ch} - P_{atm}|)}{\varrho}}\,\mathrm{sgn}(P_{ch} - P_{atm})\right) \\ &+ \left(C_D A_{lc}\sqrt{\frac{2(|P_{ld} - P_{ch}|)}{\varrho}}\,\mathrm{sgn}(P_{ld} - P_{ch})\right) - \frac{\dot{P}_{ch}}{k_{bulk}} \end{aligned} \tag{10}$$

and

$$\begin{aligned} \varepsilon_5 = (\delta D_{hm}|w_m|) &+ \left(\delta(C_D A_{chv})\sqrt{\frac{2(|P_{ch} - P_{atm}|)}{\varrho}}\right) \\ &+ \left(\delta(C_D A_{lc})\sqrt{\frac{2(|P_{ld} - P_{ch}|)}{\rho}}\right) + \frac{|\dot{P}_{ch}|}{\delta k_{bulk}} \end{aligned}$$

Upper threshold value $= rd_5 + \varepsilon_5$
Lower threshold value $= rd_5 - \varepsilon_5$ (Table 2).

Table 2 Fault signature matrix

Components	rd_1	rd_2	rd_3	rd_4	rd_5	I
D_{vp}	1	0	0	0	0	0
D_{hm}	0	0	1	1	1	1
D_{lp}	0	1	1	0	0	1
R_{vp}	1	0	0	0	0	0
R_{hm}	0	0	0	1	0	1
ν	0	0	1	0	0	1

4 Results and Discussions

For the purpose of testing the ability of this approach in successfully identifying the time-varying degradation pattern of different parameters, we intentionally introduce a fault in the volumetric displacement of the variable displacement pump, five seconds after the start of the system.

The variation of volumetric displacement of the pump with time occurs according to the following pattern (Fig. 5):

$$\begin{aligned} D_{vp} &= D_{vpn} && t < 5 \\ &= D_{vpn} * e^{-\lambda(t-5)} && 5 \leq t < 5.16095 \\ &= D_{vpn}/5 && t \geq 5.16095 \end{aligned} \tag{11}$$

Before the inception of the fault, the state equations of the variable pump (Eq. 1) take the form

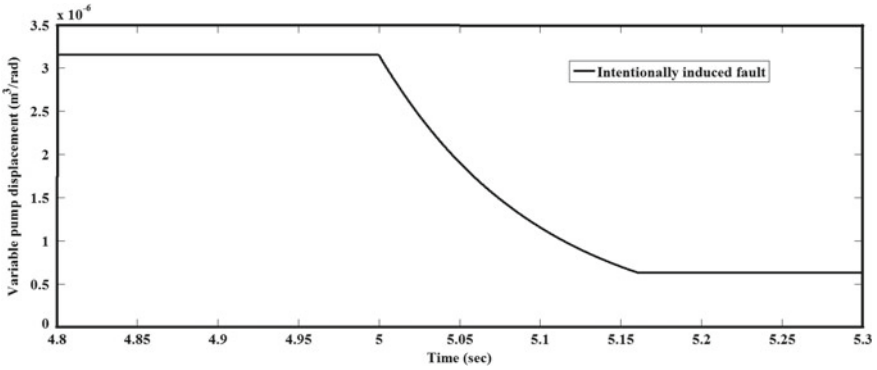

Fig. 5 Intentionally induced fault in the displacement volume of the variable displacement pump

$$Q_{\mathrm{p}} = D_{\mathrm{vp}}\omega_{\mathrm{em}} - \frac{P_{\mathrm{s}}}{R_{\mathrm{vp}}} - \left(C_{\mathrm{D}}A_{\mathrm{pv}}\sqrt{\frac{2(|P_{\mathrm{s}} - P_{\mathrm{d}}|)}{\varrho}}\mathrm{sgn}(P_{\mathrm{s}} - P_{\mathrm{d}})\right) \tag{12}$$

And residual obtained from the first phase of DBG,

$$rd_{1|1} = D_{\mathrm{vp}}\omega_{\mathrm{em}} - \frac{\dot{P}_{\mathrm{s}}}{k_{\mathrm{bulk}}} - \left(\frac{P_{\mathrm{s}}}{R_{\mathrm{vp}}}\right) - \left(C_{\mathrm{D}}A_{\mathrm{pv}}\sqrt{\frac{2(|P_{\mathrm{s}} - P_{\mathrm{d}}|)}{\varrho}}\mathrm{sgn}(P_{\mathrm{s}} - P_{\mathrm{d}})\right) \tag{13}$$

But when the inception of fault takes place, the D_{vp} becomes time variant. As a result of this, the state Eq. (12) changes to (14),

$$Q_{\mathrm{p}} = \widetilde{D_{\mathrm{vp}}}\omega_{\mathrm{em}} - \left(\frac{P_{\mathrm{s}}}{R_{\mathrm{vp}}}\right) - \left(C_{\mathrm{D}}A_{\mathrm{pv}}\sqrt{\frac{2(|P_{\mathrm{s}} - P_{\mathrm{d}}|)}{\varrho}}\mathrm{sgn}(P_{\mathrm{s}} - P_{\mathrm{d}})\right) \tag{14}$$

And residual becomes,

$$rd_{1} = \widetilde{D_{\mathrm{vp}}}\omega_{\mathrm{em}} - \frac{\dot{P}_{\mathrm{s}}}{k_{\mathrm{bulk}}} - \left(\frac{P_{\mathrm{s}}}{R_{\mathrm{vp}}}\right) - \left(C_{\mathrm{D}}A_{\mathrm{pv}}\sqrt{\frac{2(|P_{\mathrm{s}} - P_{\mathrm{d}}|)}{\varrho}}\mathrm{sgn}(P_{\mathrm{s}} - P_{\mathrm{d}})\right) \tag{15}$$

The BG model of the circuit accounting for the degradation in the volumetric displacement of the pump is given in Fig. 6.

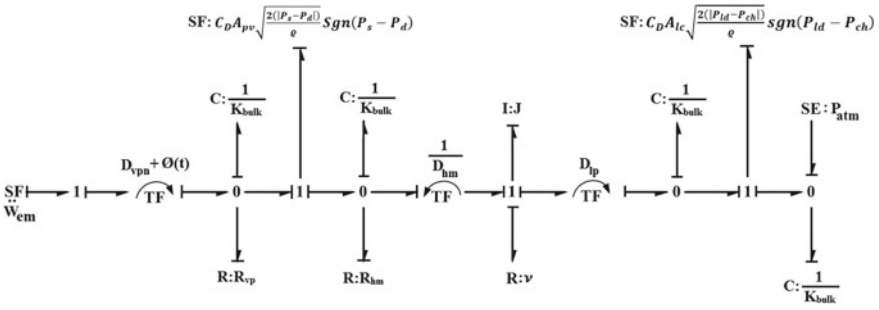

Fig. 6 Bond graph model of the hydraulic system considering the degradation pattern

As the cause for the deviation from the normal behavior of the system is the time-varying fault in the volumetric displacement of the pump so, the residual $rd_{1|1}$ deviates away from zero. As the time-varying degradation of the parameter is taken into account during the second phase of the DBG so the newly modified residual $rd_{1|2}$ approaches naught.

$$\begin{aligned} rd_{1|2} = {} & D_{\text{vpn}}\omega_{\text{em}} - \frac{\dot{P}_{\text{s}}}{k_{\text{bulk}}} - \left(\frac{P_{\text{s}}}{R_{\text{vp}}}\right) \\ & - \left(C_{\text{D}}A_{\text{pv}}\sqrt{\frac{2(|P_{\text{s}} - P_{\text{d}}|)}{\varrho}}\,\text{sgn}(P_{\text{s}} - P_{\text{d}})\right) + \varnothing(t)\omega_{\text{em}} \\ = {} & 0 \end{aligned} \tag{16}$$

or

$$rd_{1|1} = -\varnothing(t)\omega_{\text{em}}$$

or

$$\left(-\left(D_{\text{vpn}}\omega_{\text{em}} - \frac{\dot{P}_{\text{s}}}{k_{\text{bulk}}} - \left(\frac{P_{\text{s}}}{R_{\text{vp}}}\right) - \left(C_{\text{D}}A_{\text{pv}}\sqrt{\frac{2(|P_{\text{s}} - P_{\text{d}}|)}{\varrho}}\,\text{sgn}(P_{\text{s}} - P_{\text{d}})\right)\right)\Big/\omega_{\text{em}}\right) = \emptyset(t) \tag{17}$$

Herein, $\emptyset(t)$ is the unknown degradation trend and $D_{\text{vp}}(t)$ is varying displacement volume of the variable pump. $\emptyset(t)$ is the solution of (17). The overall volumetric displacement of the pump can be given by,

$$D_{\text{vp}}(t) = D_{\text{vpn}} + \emptyset(t) \tag{18}$$

The evolution of residual $rd_{1|1}$ with time is shown in Fig. 7. Table 3 contains the details of initial values given to different parameters of the system for the purpose of simulation.

The comparison between the deliberately introduced time-varying fault and the obtained degradation pattern, as shown in Fig. 8, provides the necessary evidence which supports the applicability of the approach described in this work. To help in discerning the difference between the induced degradation pattern and the recovered degradation from the Simulink model, Fig. 9 presents the enlarged view of Fig. 8 at the instant the degradation starts and Fig. 10 represents the same at the instant the degradation pattern becomes nearly constant at 5.1609 s.

Figure 11 presents that the residual $rd_{1|2}$ approaches zero if the output of the faulty system is taken as input for the ARRs.

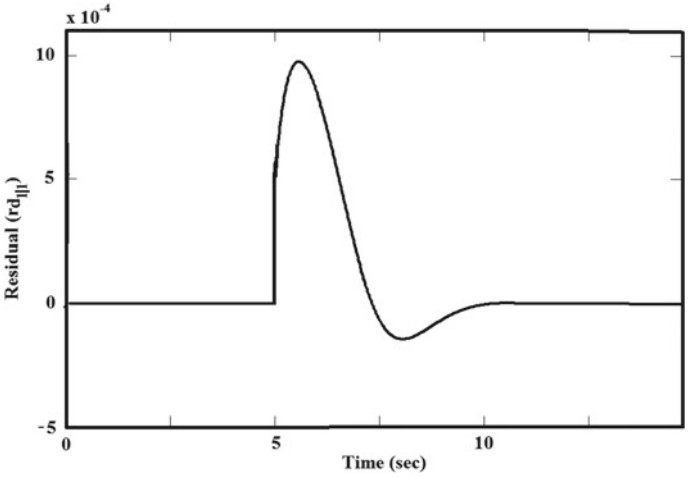

Fig. 7 Evolution of $rd_{1|1}$ with time

Table 3 Parameters of components used in simulation

Parameters	Value
Electric motor speed (ω_{em})	160 rad/s
Variable pump displacement (D_{vp})	3.15×10^{-6} m^3/rad
Bulk Stiffness (k_{bulk})	5×10^{12} N/m^2
Resistance to leakage in variable pump (R_{vp})	1.25×10^{11} N-s/m^2
Coefficient of discharge (C_D)	0.64
Density of the fluid (ϱ)	867.7 m^3/kg
Proportional valve orifice area (A_{pv})	2.25×10^{-5} m^2
Motor displacement (D_{hm})	1.91×10^{-6} m^3/rad
Inertia of motor (J)	0.012 kg m^2
Resistance to leakage in hydro motor (R_{hm})	1×10^{12} N-s/m^2
Loading pump displacement (D_{lp})	1.75×10^{-6} m^3/rad
Proportional leakage area constant for loading circuit (A_{lc})	2×10^{-5} m^2
Orifice area of check valve (A_{chv})	1.15×10^{-4} m^2
Atmospheric pressure (P_{atm})	1.01×10^5 Pa
Viscous friction (ν)	0.1 N-s/m^2
Degradation coefficient (λ)	10

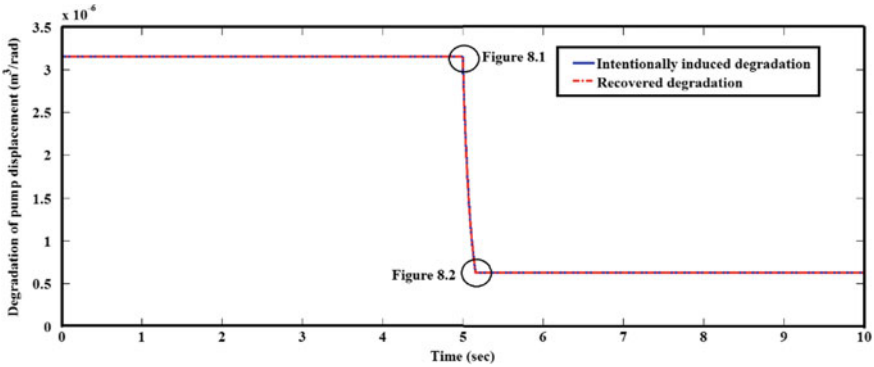

Fig. 8 Comparison between the intentionally introduced fault and the obtained degradation

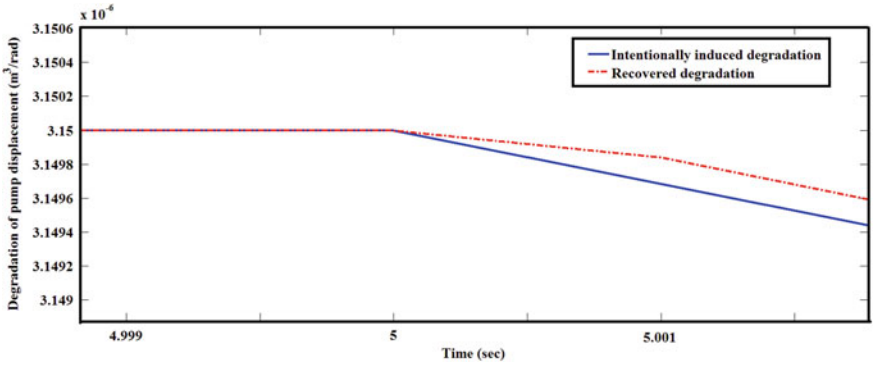

Fig. 9 Enlarged view at the instant degradation starts (i.e. at 5 s)

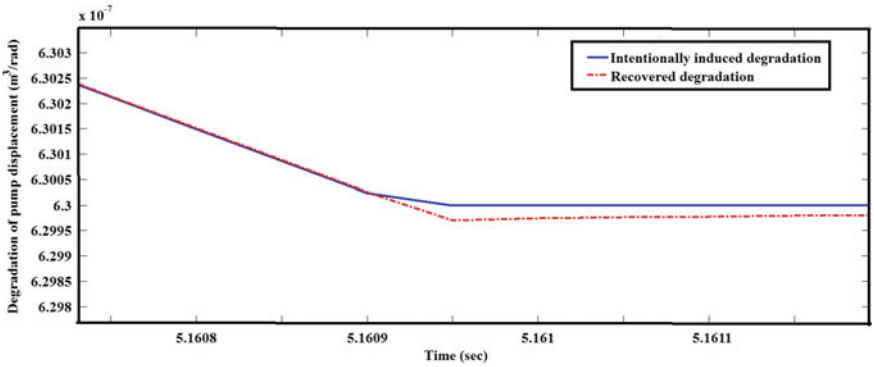

Fig. 10 Enlarged view at the instant degradation becomes constant (i.e. at 5.161 s)

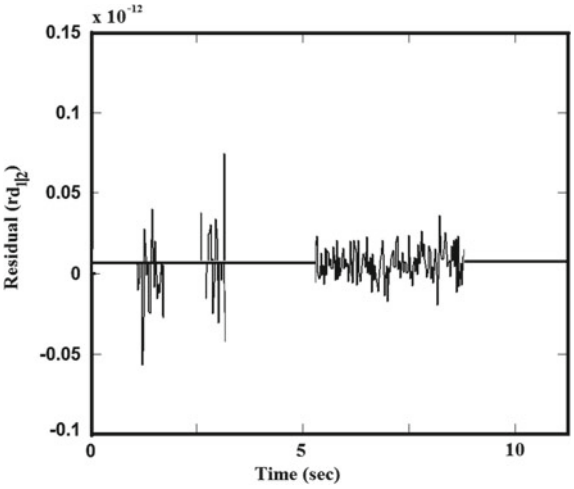

Fig. 11 Evolution of $rd_{|12}$ with time

5 Conclusions

The bond graph-based approach used in the course of this work helps to overcome the shortcomings of both model-based and data-based approach for prognosis. Using a two-phase DBG, the ARRs are established. The first-phase bond graph contributes to discerning the occurrence of fault and the second phase is utilized to determine the unknown time-varying parameter degradation with the help of the evaluated residuals. While the real system is monitored and its output signals are measured, simultaneous computation of the degradation functions is carried out. Once the time evolution of a degradation process has been computed up to some instant, an ARR residual using the values of the degradation function can be projected into the future in order to estimate the RUL. With the progression of time, repeated computation of the degradation process can be carried out resulting in improved RUL estimation.

References

1. Wu W, Hu J, Jing C, Jiang Z, Yuan S (2014) Investigation of energy efficient hydraulic hybrid propulsion system for automobiles. Energy 73:497–505
2. Lin X, Pan S, Wang D (2008) Dynamic simulation and optimal control strategy for a parallel hybrid hydraulic excavator. J Zhejiang Univ Sci A 9(5):624–632
3. Bouamama BO, Samantaray AK (2003) MSGD-T. Derivation of constraint relations from bond graph models for fault detection and isolation. In: Proceedings ICBGM'03, simulation series, vol 35, no 2. 104-109-56555-257-1
4. Samantaray AK (2017) Model-based diagnosis and prognosis of hybrid dynamical systems with dynamically updated parameters. In: Bond graphs for modelling, control and fault diagnosis of engineering systems, 2nd edn. Springer, Cham

5. Shi H, Yang H, Gong G, Liu H, Hou D (2014) Energy saving of cutterhead hydraulic drive system of shield tunneling machine. Autom Constr 37:11–21
6. Borutzky W (2018) Determination of a function for a degradation process by means of two diagnostic band graphs. IFAC-PapersOnLine 51(24):636–642
7. Kumar S, Das S, Ghoshal SK, Das J (2018) Review of different energy saving strategies applicable to hydraulic hybrid systems used in heavy vehicles. In: IOP conference series: materials science and engineering, vol 377, no 1. IOP Publishing, UK, p 012072